





Pairing dome from an emergent Feshbach resonance in a strongly repulsive bilayer model

Hannah Lange ^{1,2,3}, Lukas Homeier,^{1,3} Eugene Demler ⁴, Ulrich Schollwöck ^{1,3},
Annabelle Bohrdt,^{3,5} and Fabian Grusdt ^{1,3}

¹*Department of Physics and Arnold Sommerfeld Center for Theoretical Physics (ASC), Ludwig-Maximilians-University Munich, Theresienstr. 37, D-80333 Munich, Germany*

²*Max-Planck-Institute for Quantum Optics, Hans-Kopfermann-Str.1, D-85748 Garching, Germany*

³*Munich Center for Quantum Science and Technology, Schellingstr. 4, D-80799 Munich, Germany*

⁴*Department of Physics and Institute for Theoretical Physics, ETH Zurich, 8093 Zürich, Switzerland*

⁵*Department of Physics, University of Regensburg, Universitätsstr. 31, D-93053 Regensburg, Germany*



(Received 28 September 2023; revised 1 June 2024; accepted 29 July 2024; published 26 August 2024)

A key to understanding unconventional superconductivity lies in unraveling the pairing mechanism of mobile charge carriers in doped antiferromagnets, yielding an effective attraction between charges even in the presence of strong repulsive Coulomb interactions. Here, we study pairing in a mixed-dimensional (mixD) t - J model, featuring robust binding energies—despite dominant repulsive interactions—that are strongly enhanced in the finite doping regime. The single and coupled mixD ladders we study, corresponding to bilayers of width $w \leq 2$, feature a crossover from tightly bound pairs of holes (closed channel) at small repulsion to more spatially extended, correlated pairs of individual holes (open channel) at large repulsion. We derive an effective model for the latter, in which the attraction is mediated by the closed channel, in analogy to atomic Feshbach resonances. Using density matrix renormalization group simulations we reveal a dome of large binding energies at around 30% doping, accompanied by a change of the Fermi surface volume and a crossover from extended to tightly bound hole pairs. Our work provides a microscopic theory of pairing in the doped mixD system with dominant repulsion, closely related to bilayer, Ni-based superconductors, and our predictions can be tested in state-of-the-art quantum simulators.

DOI: [10.1103/PhysRevB.110.L081113](https://doi.org/10.1103/PhysRevB.110.L081113)

Introduction. Among the remaining mysteries of high- T_c superconductivity [1–3] is the pairing mechanism of charge carriers, leading to the formation of Cooper pairs [4] in a relatively high temperature regime and despite repulsive Coulomb interactions between the charges [5–7]. In contrast to conventional superconductors, for which BCS theory [8] predicts small pairing gaps that result in large Cooper pairs—effectively circumventing long-range Coulomb repulsion—high- T_c superconductors are characterized by their substantial pairing gap [9] and Cooper pairs are potentially exposed to extended-range Coulomb interactions. To investigate pairing mechanisms resilient to such Coulomb interactions, Fermi Hubbard or t - J type models have been extended to t - J - V models [10] with nearest-neighbor repulsion V . These models have been shown to sustain pairing up to large repulsion strengths [11,12] and have proven to effectively describe some experimental results in cuprates, e.g., on plasmon spectra [13–15]. However, such models are prohibitively difficult to solve in order to unravel the underlying pairing mechanism, despite impressive numerical advances in the past years [16–19].

Here, we study a pairing mechanism that gives rise to attractively interacting fermions despite dominant repulsion between them, with enhanced pairing in the intermediate doping regime, leading to the dome of binding energies in Fig. 1. For this purpose, we consider single and coupled ladders at high repulsion. Despite their simplicity, t - J and Fermi-Hubbard ladders have been shown to feature a variety of correlated phases [20–25], including superconduct-

ing correlations even when supplementing the models with repulsive Coulomb interactions between nearest neighbors [26,27]. Moreover, so-called mixed-dimensional (mixD) ladders, featuring hopping only along the legs but magnetic superexchange in both directions, have been shown to host binding on extremely high energy scales, even exceeding the superexchange energy [28–34]. This allows one to observe binding [32,33] and stripe formation [35,36] in these models using ultracold atom experiments [31,37–40], where experimentally reachable temperatures are today typically on the order of the superexchange energy [38]. Furthermore, recent works proposed that the high-temperature superconductor $\text{La}_3\text{Ni}_2\text{O}_7$ [41,42] can be modeled by mixD bilayers, see, e.g., Refs. [41,43–49], and might hence be closely related to the mixD bilayers of width $w = 1, 2$ studied in this work.

Here, we utilize the mixD model as a controlled setting to study the rich interplay of magnetic fluctuations, Coulomb repulsion, and arbitrary doping, see Fig. 1, with interesting emergent structures: when the half-filled ground state of a ladder with small intraleg superexchange $0 \leq J_{\parallel} \ll J_{\perp}$ is doped with a single hole, the latter can be understood as a bound state of two partons, a *chargon* and *spinon*, carrying the respective quantum numbers and connected by a linear confinement potential [31,32], as observed also in 2D [50–57]. Similarly, two holes form a pair of two chargons in the mixD setting [29,30,32–34]. In analogy to mesons in high energy physics, the constituents (*partons*) of this pair are very tightly bound and hence the chargon-chargon bound state will also be referred to as *meson* in the following. In this Letter we show that

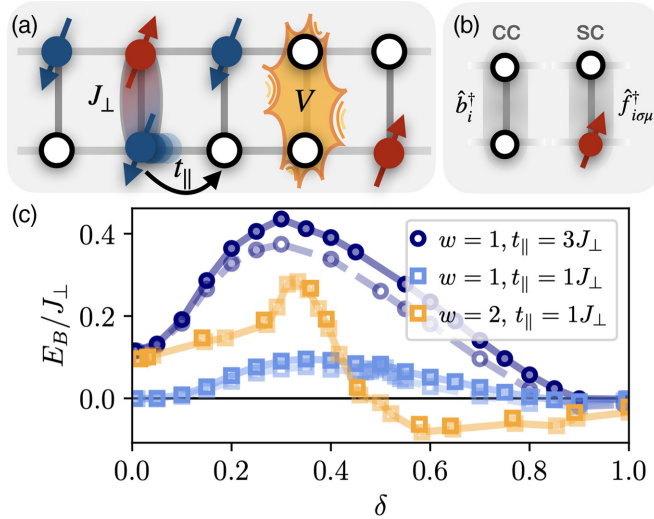


FIG. 1. (a) Schematic picture of the mixD ladder, with exchange coupling J_{\perp} between the legs, hopping t_{\parallel} only along the legs, and repulsion V between holes on the same rung. (b) The constituents of the effective theory in the large V limit: charge-charge (cc) pairs $\hat{b}_i^{(\dagger)}$ and spinon-chargeon (sc) pairs $\hat{f}_{i\sigma\mu}^{(\dagger)}$. (c) Binding energies with respect to hole doping δ for $V/J_{\perp} = 5$, for ladders (blue) with $L_x = 100(200)$, and bilayers of width $w = 2$ (orange) with $L_x = 24(32)$ [dashed (solid) lines].

strong interactions—approximating the Coulomb repulsion of electrons in solids—favor another pairing scenario which, we argue, is more closely related to the pairing seen in most real materials: more extended Cooper-type bound states of two mesons, i.e., consisting of four constituents (*tetrapartons*).

Specifically, we investigate mixD t - J bilayers of width $w = 1, 2$, i.e., single and coupled ladders, supplemented with strong repulsive interactions V between two holes on a rung [see Fig. 1(a)]—i.e., an off-site repulsion that may also be relevant in bilayer nickelate superconductors. Combining density matrix renormalization group (DMRG) simulations [58,59], including the calculation of angle resolved photoemission spectroscopy (ARPES) spectra, and effective descriptions in terms of the emergent charge carriers, we show that the effective attraction between the holes in the large V regime is induced by coupling processes to the chargeon-chargeon, mesonlike states, leading to a dome of binding energies in the intermediate doping regime. To highlight the analogy of this mechanism to Feshbach resonances [60], we refer to the high energy channel of chargeon-chargeon (cc) states as a closed, mesonic channel and to the low energy spinon-chargeon (sc) pairs as the open, tetraparton channel at large V .

Overall, despite their simplicity, the mixD systems we study show some remarkable phenomenological similarities with strongly correlated superconductors such as cuprates and bilayer nickelates: (i) we report pairing facilitated by doping, leading to a dome of binding energies with its peak at 30% doping [see Fig. 1(c)]; (ii) the pairing we find only requires short-range antiferromagnetic (AFM) correlations but no long-range magnetic order; (iii) we observe a change of the Fermi surface volume, similar to the small-to-large Fermi surface transition in cuprates; (iv) we discover a density wave (with bond order) in the intermediate doping regime [61].

Model and emergent constituents. The primary goal of this work is to investigate the impact of strong repulsive interactions V on the pairing mechanism in a mixD system, featuring interlayer exchange interactions but no interlayer tunneling [28,32,33]; see Fig. 1(a):

$$\hat{\mathcal{H}} = -t_{\parallel} \hat{\mathcal{P}} \sum_{(ij)} \sum_{\mu, \sigma} (\hat{c}_{i\mu\sigma}^{\dagger} \hat{c}_{j\mu\sigma} + \text{H.c.}) \hat{\mathcal{P}} + J_{\perp} \sum_j \left(\hat{S}_{j0} \cdot \hat{S}_{j1} - \frac{1}{4} \hat{n}_{j0} \hat{n}_{j1} \right) + V \sum_j \hat{n}_{j0}^h \hat{n}_{j1}^h. \quad (1)$$

Here, $\hat{\mathcal{P}}$ is the Gutzwiller projector onto the subspace with maximum single occupancy per site. Spin operators at site j in layer $\mu = 0, 1$ are denoted by $\hat{S}_{j\mu}$, (hole) density operators by $\hat{n}_{j\mu} = \hat{n}_{j\mu\uparrow} + \hat{n}_{j\mu\downarrow}$ ($\hat{n}_{j\mu}^h = 1 - \hat{n}_{j\mu}$), and $\hat{c}_{j\mu\sigma}$ annihilate a fermion with spin $\sigma = \uparrow, \downarrow$.

At half filling, the ground state of the system is given by spin singlets on each rung [32]. At finite doping, the system is dominated by a competition of kinetic energy and the energy of the distortion of the spin background when holes move. The emergent constituents in this doping regime are most easily understood when $t_{\parallel} \ll J_{\perp}$. At $V = 0 \leq t_{\parallel} \ll J_{\perp}$ two holes tend to sit on the same rung—a configuration with energy $-J_{\perp}$ —and form a chargeon-chargeon pair (cc); see Fig. 1(b), left. They can move freely through the system, since the second chargeon restores the spin-singlet background when following the first one, making it favorable for charges to move through the system together, i.e., yielding large binding energies [32]. When the repulsive interaction V reaches a critical value V_c , it is energetically favorable to place at maximum one hole (and one spin) per rung, i.e., to form a spinon-chargeon pair (sc); see Fig. 1(b), right. In contrast to cc's, the motion of sc's is suppressed by the distortion of the singlet spin background created when the chargeon moves.

When $t_{\parallel} > J_{\perp}$, this meson picture remains qualitatively correct, although the cc's and sc's develop a finite spatial extent determined by the interplay of the kinetic energy and a linear confining potential (a *string*) between the partons [32,56]; see also [61]. As we show in the following sections, the crossover from the cc ($V < V_c$) to the sc regime ($V > V_c$) depends strongly on the ratio t_{\parallel}/J_{\perp} , i.e., $V_c = V_c(t_{\parallel}/J_{\perp})$.

Limits of low and high doping. Using the DMRG package SYTEN [63,64] with $U(1)_{N_{\mu=1,2}}$ symmetry on each layer and global $U(1)_{S^{\text{tot}}}$ symmetry, we calculate the binding energies,

$$E_B(N_h) = 2(E_{N_h-1} - E_{N_h-2}) - (E_{N_h} - E_{N_h-2}), \quad (2)$$

where N_h is the number of holes doped in the system and $E_B > 0$ indicates binding of holes. Details on the implementation can be found in [61].

Our results in the limits of very low ($N_h = 2$) and high ($N_p = L_x \cdot L_y - N_h = 2$) doping are shown in Fig. 2. For $t_{\parallel} = 0$ the cc at low doping and the particle pair at high doping are bound by the fact that it is energetically favorable to form singlets on the rungs. In both cases, the pairs unbind when $V \geq V_c(t_{\parallel} = 0) = J_{\perp}$.

For $t_{\parallel} \ll J_{\perp}$ we perform a Schrieffer-Wolff transformation, as detailed further below, to estimate the critical value V_c , where the nature of the constituents changes from tightly

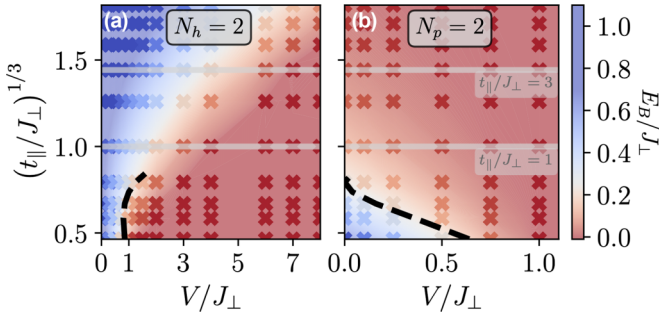


FIG. 2. Binding energy in the limits of (a) low ($N_h = 2$) and (b) high ($N_p = L_x \cdot L_y - N_h = 2$) doping. If $t_{\parallel} \ll V, J_{\perp}$ the critical V_c values for which cc's do not constitute the ground state any more are denoted by the black dotted lines (see [62]). Here, we expect the crossover to the sc regime. For large t_{\parallel}/J_{\perp} and $V = 0$ binding energies are proportional to $t_{\parallel}^{1/3}$ [32].

bound cc's to weakly bound sc's in the low and high hole doping regimes [31]; see [62]. The resulting perturbative expressions for V_c , indicated by the dashed black lines in Fig. 2, agree well with the numerical results for $t_{\parallel} \leq J_{\perp}$. At low doping, Fig. 2(a), even the backbending observed numerically is captured correctly. Furthermore, analytics and numerics show that the low and high doping regimes are distinctly different. (a) For two holes, the string-based pairing mechanism [32] yields pronounced binding even for large t_{\parallel}/J_{\perp} . For example, for $t_{\parallel}/J_{\perp} = 3$, a repulsion $V > 7J_{\perp}$ is needed to suppress the binding energy below $E_B/J_{\perp} = 10\%$, coinciding with the numerical observation of widely spread hole pairs over more than 20 sites for a system of length $L_x = 80$ (see [61]). (b) In the high doping limit with only two particles remaining in the system, the binding energy is suppressed to very small values $E_B/J_{\perp} < 0.01$ as soon as $V \lesssim J_{\perp}$. For large $t_{\parallel} \geq J_{\perp}$, the perturbative description breaks down.

Strong pairing at finite doping. For large V , we show in Figs. 1(c) and 2 that neither very low nor very high doping permits significant pairing of charges. Remarkably, we find drastically enhanced binding energies at intermediate doping values in single and coupled ladders in Fig. 1(c), where $V = 5J_{\perp}$: in all cases, E_B shows a pronounced dome around $\delta_{\text{opt}} \approx 30\%$ doping, before decreasing again down to a vanishingly small or even negative value for the two-particle system. For ladders, binding is increased from a vanishingly small value (substantial value) for $t_{\parallel}/J_{\perp} = 1$ ($t_{\parallel}/J_{\perp} = 3$) by a factor > 10 (3) in the finite doping regime. The same behavior can be observed for bilayers of width $w = 2$, but with larger binding energies in the low doping regime. This can be understood by the fact that, in 2D, the chargon moves on a Bethe lattice, renormalizing the hopping to $t \rightarrow \sqrt{2}t \approx 1.7t$ [55] and stabilizing the binding as explained above.

To gain a better understanding of the binding energies in the finite doping regime we derive an effective model for $V > t_{\parallel}, J_{\perp}$ —a regime for which sc configurations are dominant. In this limit of large $V > J_{\perp} \gg t_{\parallel}$ we identify two subspaces of (i) sc constituents at low energy and (ii) cc configurations that are gapped by $\Delta E = V - J_{\perp}$. We perform a Schrieffer-Wolff transformation [65] of Eq. (1) assuming small $|t_{\parallel}/\Delta E|$ and integrate out the cc states; see the Supplemental Material (SM) [62]. We express the effective Hamiltonian in terms

of sc operators $\hat{f}_{i\mu\sigma}^{(\dagger)}$, acting on the vacuum state consisting of rung singlets. At $V > J_{\perp} \gg t_{\parallel}$ at maximum one sc is allowed per rung, which we enforce by the projector $\hat{\mathcal{P}}_f$ on the corresponding subspace. Moreover, the effective Hamiltonian only applies below $\delta \leq 50\%$ doping, before cc's naturally proliferate. We find (see [61])

$$\begin{aligned} \hat{\mathcal{H}}_{\text{eff}}^{\text{sc}} = & \frac{t_{\parallel}}{2} \sum_j \sum_{\sigma, \mu} \hat{\mathcal{P}}_f (\hat{f}_{j+1\mu\sigma}^{\dagger} \hat{f}_{j\mu\sigma} + \text{H.c.}) \hat{\mathcal{P}}_f \\ & + \epsilon_0 \sum_{j\mu} \hat{n}_{j\mu}^f + \frac{t_{\parallel}^2}{J_{\perp}} \frac{3}{2} \sum_j \sum_{\mu\mu'} \hat{n}_{j+1\mu}^f \hat{n}_{j\mu'}^f \\ & - 4t_{\parallel}^2 \sum_j \left(-\hat{\mathbf{J}}_{j+1} \cdot \hat{\mathbf{J}}_j + \frac{1}{4} \right) \left[\frac{\hat{\mathcal{P}}_j^S}{V - J_{\perp}} + \frac{\hat{\mathcal{P}}_j^T}{V} \right]. \end{aligned} \quad (3)$$

Here, we have defined $\epsilon_0 = J_{\perp} - \frac{t_{\parallel}^2}{J_{\perp}} \frac{3}{2}$ and the singlet and triplet projectors $\hat{\mathcal{P}}_j^S = -\hat{\mathbf{S}}_{j+1} \cdot \hat{\mathbf{S}}_j + \frac{1}{4} \hat{n}_{j+1}^f \hat{n}_j^f$ and $\hat{\mathcal{P}}_j^T = \hat{\mathbf{S}}_{j+1} \cdot \hat{\mathbf{S}}_j + \frac{3}{4} \hat{n}_{j+1}^f \hat{n}_j^f$, with the sc density operators $\hat{n}_{j\mu}^f = \sum_{\sigma} \hat{f}_{j\mu\sigma}^{\dagger} \hat{f}_{j\mu\sigma}$, the sc spin operators $\hat{\mathbf{S}}_j = \frac{1}{2} \sum_{\mu} \sum_{\sigma\sigma'} \hat{f}_{j\mu\sigma}^{\dagger} \boldsymbol{\sigma}_{\sigma\sigma'} \hat{f}_{j\mu\sigma'}$, and isospin leg operators

$$\hat{\mathbf{J}}_j = \frac{1}{2} \sum_{\sigma} \sum_{\mu\mu'} \hat{f}_{j\mu\sigma}^{\dagger} \boldsymbol{\sigma}_{\mu\mu'} \hat{f}_{j\mu'\sigma}. \quad (4)$$

Equation (3) describes hard-core, fermionic sc's, experiencing repulsive (third term) and attractive interactions $\propto \frac{t_{\parallel}^2}{V - J_{\perp}}$ and $\propto \frac{t_{\parallel}^2}{V}$ (fourth term with negative sign for spin singlet/triplet configurations and leg singlets) that compete with each other. We emphasize that the attraction is mediated by virtual processes involving the high-energy cc channel shown in the SM [62], Fig. 1(a), similar to the attraction induced at a Feshbach resonance. This is also apparent from the term $\propto \hat{\mathbf{J}}_{j+1} \cdot \hat{\mathbf{J}}_j$, which penalizes neighboring sc's occupying the same leg, since only sc's from opposite legs can lower their energy by recombining virtually into the cc channel. Furthermore, a resonance occurs at $V \rightarrow J_{\perp}$, where the attractive interaction diverges and becomes dominant over the repulsion.

The Feshbach-mediated pairing mechanism in Eq. (3) is in qualitative agreement with the doping dependence of the binding energies of the mixD bilayers with $w = 1, 2$ in Fig. 1(c) and is in principle even valid for the full 2D limit $w \rightarrow \infty$. Near the resonance, when the attraction is dominant, the attractive interactions predicted by Eq. (3) are effectively enhanced when the number of holes in the system is increased, since the kinetic energy per hole decreases with doping (Pauli pressure). This suggests an increasing binding energy with doping, i.e., when the number of sc's increases, similar to the dome of E_B in Fig. 1(c). The optimal doping δ_{opt} , corresponding to maximum binding energy, is reached when sc's begin to overlap spatially: in the effective model (3) of pointlike sc's, this suggests a maximum at $\delta_{\text{opt}} = 50\%$, in agreement with our numerical results on the full mixD system as well as on the effective sc model for $t_{\parallel} \ll J_{\perp}$ [61]. For larger $t_{\parallel} \geq J_{\perp}$, we expect that the mechanism remains essentially the same, but with two main changes: (i) since binding is stabilized by t_{\parallel} , the resonance shifts to higher values $V_c > J_{\perp}$, yielding positive

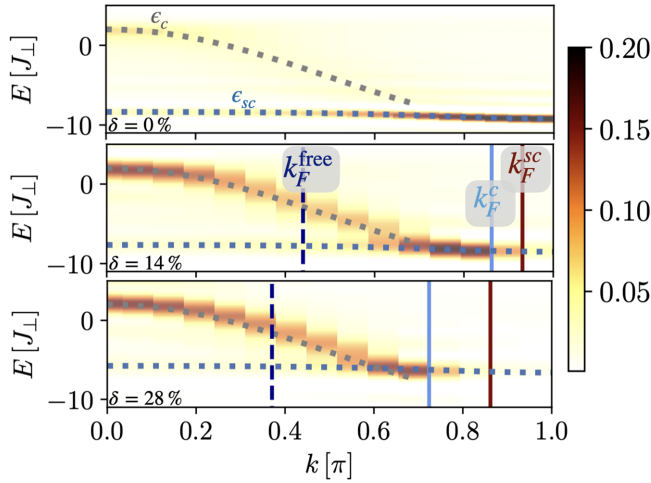


FIG. 3. ARPES spectra at $\delta = 0, 0.14, 0.28$ (top to bottom) and for $V/J_{\perp} = 5$, $t_{\parallel}/J_{\perp} = 3$. Furthermore, we show eigenenergies of free sc's, ϵ_c , and sc's, ϵ_{sc} , from geometric string theory [32] (dotted lines), as well as Fermi momenta for free fermions k_F^{free} , free chargons k_F^c , and sc pairs k_F^{sc} . Both k_F^c and k_F^{sc} coincide with an onset of spectral weight in the finite doping regime.

binding energies even for large $V = 5J_{\perp}$ at finite doping that are on the same order of magnitude as in Fig. 1; see [61]; (ii) sc's extend over several rungs and δ_{opt} shifts to smaller values $< 50\%$; see Fig. 1(c).

Another remarkable feature of the effective model (3) is the emergent isospin $SU(2)$ symmetry. We find numerical indications that this $SU(2)$ symmetry is only approximately present in the full mixD system (1), see [62], with a strong doping dependence; see also [61]. When higher orders in $t_{\parallel}/\Delta E$ are considered, the $SU(2)$ isospin symmetry of Eq. (3) breaks down.

ARPES spectra. In Fig. 3 the ARPES spectra upon removing a single hole from the mixD ladder at $\delta = 0$ (top), $\delta = 0.14$ (middle), and $\delta = 0.28$ (bottom) hole doping, focusing on high repulsion $V/J_{\perp} = 5$, are shown (see the SM [62], Sec. 4, and Refs. [66,67] therein). At low doping, the low-energy spectrum is dominated by a narrow band, matching the dispersion of sc's ϵ_{sc} calculated from geometric string theory as in [32]. For larger δ , the spectral weight continuously shifts into a more dispersive, higher energy branch that matches the dispersion of free particles, $\epsilon_c = 2t \cos(k)$. Furthermore, the onset of the spectral weight, indicating the Fermi momentum of the system, changes from a small momentum to a large one with doping: at low doping, the onset matches the sc Fermi momentum $k_F^{\text{sc}} = \frac{1}{4}\pi n_{sc}$ with $n_{sc} = N_h/L_x$, where the factor $1/4$ accounts for layer and spin indices of sc's. At larger δ , a second onset of spectral weight at $k_F^c = \pi n_c$ becomes apparent, which can be associated with free, spinless chargons with density $n_c = \delta$. Hence our results indicate a change of the Fermi surface volume around δ_{opt} [48], similar to the phenomenology of cuprates [68]. The momentum of free, spinful fermions $k_F^{\text{free}} = \frac{1}{2}\pi(1 - \delta)$ does not match the onset of the spectral weight in any case.

Experimental realizations. Our studies are motivated by recent experiments in cold atoms and bilayer nickelate compounds.

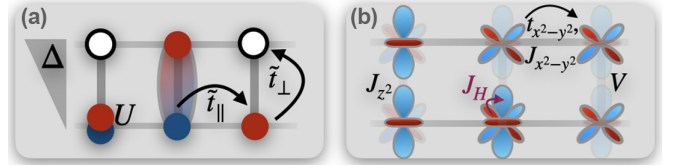


FIG. 4. (a) Ultracold atom setup for a mixD ladder with repulsion: a potential offset Δ and hole (doublon) doping in the upper (lower) leg are applied. (b) Schematic illustration of the bilayer $\text{La}_3\text{Ni}_2\text{O}_7$: $d_{x^2-y^2}$ orbitals contribute to intralayer hopping and AFM exchange, d_z^2 orbitals to an interlayer AFM exchange and both orbitals are coupled by FM Hund's coupling J_H .

The mixD ladder without repulsion V was already realized in a setup of ultracold fermionic atoms in an optical potential [33] by applying a potential offset Δ between the legs to suppress the interleg tunneling \tilde{t}_{\perp} to an effective $t_{\perp} \approx 0$. To supplement this setup with a nearest-neighbors repulsion, we propose hole (doublon) doping for upper (lower) legs of the ladder; see Fig. 4(a). This gives rise to virtual hopping processes between doublons in the lower leg and holes in the upper leg with amplitude $2\frac{\tilde{t}_{\perp}^2}{\Delta}$ and doublons and spins with $\frac{\tilde{t}_{\perp}^2}{\Delta+U}$, yielding a total interaction strength $V = 2\tilde{t}_{\perp}^2 \frac{U}{\Delta(U-\Delta)}$ [61].

Furthermore, as discussed in [44], the recently discovered bilayer nickelate superconductor $\text{La}_3\text{Ni}_2\text{O}_7$ [41] can be modeled by a $t_{\parallel} - J_{\parallel} - J_{\perp}$ bilayer similar to the model we study. In this material, the $d_{x^2-y^2}$ orbitals form an effective intralayer $t_{x^2-y^2} - J_{x^2-y^2}$ model, whereas the d_z^2 orbitals are localized with interlayer antiferromagnetic (AFM) superexchange; see Fig. 4(b). Both orbitals interact via ferromagnetic (FM) Hund's coupling J_H . In the limit of sizable $|J_H|$ the spins of $d_{x^2-y^2}$ and d_z^2 form triplets, giving rise to an effective AFM interaction J_{\perp} of $d_{x^2-y^2}$ spins between the layers [44,45]. In contrast to AFM interactions solely originating from superexchange, the interaction mediated via Hund's rule yields vanishingly small interlayer hopping. We argue that in such a 2D material the Coulomb repulsion V may play an important role at low doping. Our numerical results for increasing width w of the bilayers and the effective model (3), which is also valid in the 2D limit $w \rightarrow \infty$, suggest that, in such a 2D bilayer system, Feshbach-mediated pairing is a possible scenario [69]. In the BEC regime, similar effective models to Eq. (3) have proven to provide an insightful perspective into the underlying physics in two dimensions [49].

Summary and outlook. Our results show that effective attractive interactions between charge carriers can arise even in the presence of strong repulsive interactions, here in the setting of single and coupled mixD t - J ladders, corresponding to bilayers of width $w = 1, 2$. The binding energies we obtain feature a pronounced maximum (pairing dome) in the intermediate doping regime at strong repulsion, where the system can be understood in terms of correlated sc's [(sc) 2].

The state that we observe is a Luther-Emery liquid of (sc) 2 pairs with no charge gap but a spin gap, except for a bond-ordered density wave at $\delta = 50\%$, which we discuss in [61]. Similar to works on atomic BEC-BCS crossovers (e.g., Refs. [70–73]), where binding in the Luther-Emery state is in-

duced by a narrow Feshbach resonance with a closed channel of bosonic molecules [73], our mixD model results suggest that binding in the $(sc)^2$ regime arises from coupling to the closed cc channel. Furthermore, our spectroscopic analysis shows that a change from a small to large Fermi surface occurs in the intermediate doping regime, which can be associated with sc 's and free chargons, respectively.

Finally, our results may have implications for understanding pairing in high- T_c cuprate compounds [69] and recently discovered bilayer Ni-based superconductors [41]. In the context of the latter, our model can be seen as an extension of previously studied mixD $t_{\parallel}-J_{\parallel}-J_{\perp}$ models [43–47] to finite-range Coulomb repulsion that should also be present in these materials. Extending our analysis to truly 2D bilayers with $w > 2$ at finite doping will be an important step towards a microscopic description of the underlying pairing mechanism in these materials.

Note added. Recently, we became aware of a closely related work by Yang *et al.* [48], in which they use DMRG to study a similar repulsive t - J model on a two-leg ladder. In their

work, they also find the emergence of Feshbach resonance and propose a doping induced BEC-to-BCS crossover scenario for the bilayer nickelates.

Acknowledgments. We would like to thank A. Imamoglu, D. Jirovec, F. Palm, H. Schlömer, I. Bloch, I. Morera Navarro, L. Vandersypen, M. Greiner, M. Kebric, P. Cova Farina, T. Harris, and T. Blatz for helpful discussions. Special thanks to H. Schlömer for his help with the DMRG implementation of the mixD symmetries. We acknowledge funding by the Deutsche Forschungsgemeinschaft (DFG, German Research Foundation) under Germany's Excellence Strategy—EXC-2111—390814868 and from the European Research Council (ERC) under the European Union's Horizon 2020 research and innovation program (Grant Agreement No. 948141)—ERC Starting Grant SimUcQuam. E.D. acknowledges support from the ARO Grant No. W911NF-20-1-0163 and the SNSF Project No. 200021-212899. H.L. acknowledges support by the International Max Planck Research School for Quantum Science and Technology. L.H. acknowledges support by Studienstiftung des deutschen Volkes.

-
- [1] J. G. Bednorz and K. A. Müller, Possible high- T_c superconductivity in the Ba-La-Cu-O system, *Z. Phys. B* **64**, 189 (1986).
- [2] P. A. Lee, N. Nagaosa, and X.-G. Wen, Doping a Mott insulator: Physics of high-temperature superconductivity, *Rev. Mod. Phys.* **78**, 17 (2006).
- [3] D. J. Scalapino, Superconductivity and spin fluctuations, *J. Low Temp. Phys.* **117**, 179 (1999).
- [4] L. N. Cooper, Bound electron pairs in a degenerate Fermi gas, *Phys. Rev.* **104**, 1189 (1956).
- [5] W. Kohn and J. M. Luttinger, New mechanism for superconductivity, *Phys. Rev. Lett.* **15**, 524 (1965).
- [6] A. Kantian, M. Dolfi, M. Troyer, and T. Giamarchi, Understanding repulsively mediated superconductivity of correlated electrons via massively parallel density matrix renormalization group, *Phys. Rev. B* **100**, 075138 (2019).
- [7] S. Chakravarty and S. A. Kivelson, Electronic mechanism of superconductivity in the cuprates, c_{60} , and polyacenes, *Phys. Rev. B* **64**, 064511 (2001).
- [8] J. Bardeen, Theory of the meissner effect in superconductors, *Phys. Rev.* **97**, 1724 (1955).
- [9] M. Hashimoto, I. M. Vishik, R.-H. He, T. P. Devereaux, and Z.-X. Shen, Energy gaps in high-transition-temperature cuprate superconductors, *Nat. Phys.* **10**, 483 (2014).
- [10] L. F. Feiner, J. H. Jefferson, and R. Raimondi, Effective single-band models for the high- T_c cuprates. I. Coulomb interactions, *Phys. Rev. B* **53**, 8751 (1996).
- [11] Q.-H. Wang, J. H. Han, and D.-H. Lee, Pairing near the Mott insulating limit, *Phys. Rev. B* **65**, 054501 (2001).
- [12] L. Zinni, M. Bejas, and A. Greco, Superconductivity with and without glue and the role of the double-occupancy forbidding constraint in the t - J - V model, *Phys. Rev. B* **103**, 134504 (2021).
- [13] M. Hepting, T. D. Boyko, V. Zimmermann, M. Bejas, Y. E. Suyolcu, P. Puphal, R. J. Green, L. Zinni, J. Kim, D. Casa, M. H. Upton, D. Wong, C. Schulz, M. Bartkowiak, K. Habicht, E. Pomjakushina, G. Cristiani, G. Logvenov, M. Minola, H. Yamase *et al.*, Evolution of plasmon excitations across the phase diagram of the cuprate superconductor $\text{La}_{2-x}\text{Sr}_x\text{CuO}_4$, *Phys. Rev. B* **107**, 214516 (2023).
- [14] A. Greco, H. Yamase, and M. Bejas, Plasmon excitations in layered high- T_c cuprates, *Phys. Rev. B* **94**, 075139 (2016).
- [15] A. Greco, H. Yamase, and M. Bejas, Origin of high-energy charge excitations observed by resonant inelastic x-ray scattering in cuprate superconductors, *Commun. Phys.* **2**, 3 (2019).
- [16] M. Qin, C.-M. Chung, H. Shi, E. Vitali, C. Hubig, U. Schollwöck, S. R. White, and S. Zhang (Simons Collaboration on the Many-Electron Problem), Absence of superconductivity in the pure two-dimensional Hubbard model, *Phys. Rev. X* **10**, 031016 (2020).
- [17] T. Schäfer, N. Wentzell, F. Šimkovic, Y.-Y. He, C. Hille, M. Klett, C. J. Eckhardt, B. Arzhang, V. Harkov, F.-M. Le Régent, A. Kirsch, Y. Wang, A. J. Kim, E. Kozik, E. A. Stepanov, A. Kauch, S. Andergassen, P. Hansmann, D. Rohe, Y. M. Vilk *et al.*, Tracking the footprints of spin fluctuations: A multi-method, multimessenger study of the two-dimensional Hubbard model, *Phys. Rev. X* **11**, 011058 (2021).
- [18] H. Xu, C.-M. Chung, M. Qin, U. Schollwöck, S. R. White, and S. Zhang, Coexistence of superconductivity with partially filled stripes in the Hubbard model, *Science* **384**, eadh7691 (2024).
- [19] D. P. Arovas, E. Berg, S. A. Kivelson, and S. Raghu, The Hubbard model, *Annu. Rev. Condens. Matter Phys.* **13**, 239 (2022).
- [20] E. Dagotto, J. Riera, and D. Scalapino, Superconductivity in ladders and coupled planes, *Phys. Rev. B* **45**, 5744 (1992).
- [21] M. Sigrist, T. M. Rice, and F. C. Zhang, Superconductivity in a quasi-one-dimensional spin liquid, *Phys. Rev. B* **49**, 12058 (1994).
- [22] Z. Zhu, H.-C. Jiang, D. N. Sheng, and Z.-Y. Weng, Nature of strong hole pairing in doped Mott antiferromagnets, *Sci. Rep.* **4**, 5419 (2014).

- [23] Y.-H. Zhang and A. Vishwanath, Pair-density-wave superconductor from doping haldane chain and rung-singlet ladder, *Phys. Rev. B* **106**, 045103 (2022).
- [24] H.-K. Zhang, R.-Y. Sun, and Z.-Y. Weng, Pair density wave characterized by a hidden string order parameter, *Phys. Rev. B* **108**, 115136 (2023).
- [25] H.-C. Jiang, S. Chen, and Z.-Y. Weng, Critical role of the sign structure in the doped Mott insulator: Luther-Emery versus Fermi-liquid-like state in quasi-one-dimensional ladders, *Phys. Rev. B* **102**, 104512 (2020).
- [26] E. Dagotto and J. Riera, Superconductivity in the two-dimensional $t - J$ model, *Phys. Rev. B* **46**, 12084 (1992).
- [27] M. Troyer, Simulation of constrained fermions in low-dimensional systems, Ph.D. thesis, ETH Zurich, 1994.
- [28] F. Grusdt, Z. Zhu, T. Shi, and E. Demler, Meson formation in mixed-dimensional $t - J$ models, *SciPost Phys.* **5**, 057 (2018).
- [29] S. Chen, Z. Zhu, and Z.-Y. Weng, Two-hole ground state wavefunction: Non-BCS pairing in a $t - j$ two-leg ladder, *Phys. Rev. B* **98**, 245138 (2018).
- [30] Z. Zhu, D. N. Sheng, and Z.-Y. Weng, Pairing versus phase coherence of doped holes in distinct quantum spin backgrounds, *Phys. Rev. B* **97**, 115144 (2018).
- [31] A. Bohrdt, L. Homeier, C. Reinmoser, E. Demler, and F. Grusdt, Exploration of doped quantum magnets with ultracold atoms, *Ann. Phys. (NY)* **435**, 168651 (2021), special issue on Philip W. Anderson.
- [32] A. Bohrdt, L. Homeier, I. Bloch, E. Demler, and F. Grusdt, Strong pairing in mixed-dimensional bilayer antiferromagnetic Mott insulators, *Nat. Phys.* **18**, 651 (2022).
- [33] S. Hirthe, T. Chalopin, D. Bourgund, P. Bojović, A. Bohrdt, E. Demler, F. Grusdt, I. Bloch, and T. A. Hilker, Magnetically mediated hole pairing in fermionic ladders of ultracold atoms, *Nature (London)* **613**, 463 (2023).
- [34] H.-C. Jiang, Z.-X. Li, A. Seidel, and D.-H. Lee, Symmetry protected topological luttinger liquids and the phase transition between them, *Sci. Bull.* **63**, 753 (2018).
- [35] H. Schlämer, A. Bohrdt, L. Pollet, U. Schollwöck, and F. Grusdt, Robust stripes in the mixed-dimensional $t - J$ model, *Phys. Rev. Res.* **5**, L022027 (2023).
- [36] D. Bourgund, T. Chalopin, P. Bojović, H. Schlämer, S. Wang, T. Franz, S. Hirthe, A. Bohrdt, F. Grusdt, I. Bloch, and T. A. Hilker, Formation of stripes in a mixed-dimensional cold-atom Fermi-Hubbard system, [arXiv:2312.14156](https://arxiv.org/abs/2312.14156).
- [37] R. A. Hart, P. M. Duarte, T.-L. Yang, X. Liu, T. Paiva, E. Khatami, R. T. Scalettar, N. Trivedi, D. A. Huse, and R. G. Hulet, Observation of antiferromagnetic correlations in the Hubbard model with ultracold atoms, *Nature (London)* **519**, 211 (2015).
- [38] A. Mazurenko, C. S. Chiu, G. Ji, M. F. Parsons, M. Kánász-Nagy, R. Schmidt, F. Grusdt, E. Demler, D. Greif, and M. Greiner, A cold-atom Fermi-Hubbard antiferromagnet, *Nature (London)* **545**, 462 (2017).
- [39] I. Bloch, J. Dalibard, and W. Zwerger, Many-body physics with ultracold gases, *Rev. Mod. Phys.* **80**, 885 (2008).
- [40] C. Gross and I. Bloch, Quantum simulations with ultracold atoms in optical lattices, *Science* **357**, 995 (2017).
- [41] H. Sun, M. Huo, X. Hu, J. Li, Z. Liu, Y. Han, L. Tang, Z. Mao, P. Yang, B. Wang, J. Cheng, D.-X. Yao, G.-M. Zhang, and M. Wang, Signatures of superconductivity near 80 k in a nickelate under high pressure, *Nature (London)* **621**, 493 (2023).
- [42] Y. Zhang, D. Su, Y. Huang, Z. Shan, H. Sun, M. Huo, K. Ye, J. Zhang, Z. Yang, Y. Xu, Y. Su, R. Li, M. Smidman, M. Wang, L. Jiao, and H. Yuan, High-temperature superconductivity with zero resistance and strange-metal behaviour in $\text{La}_3\text{Ni}_2\text{O}_{7-\delta}$, *Nat. Phys.* **20**, 1269 (2024).
- [43] W. Wú, Z. Luo, D.-X. Yao, and M. Wang, Superexchange and charge transfer in the nickelate superconductor $\text{La}_3\text{Ni}_2\text{O}_7$ under pressure, *Sci. China Phys. Mech. Astron.* **67**, 117402 (2024).
- [44] C. Lu, Z. Pan, F. Yang, and C. Wu, Interlayer coupling driven high-temperature superconductivity in $\text{La}_3\text{Ni}_2\text{O}_7$ under pressure, *Phys. Rev. Lett.* **132**, 146002 (2024).
- [45] X.-Z. Qu, D.-W. Qu, J. Chen, C. Wu, F. Yang, W. Li, and G. Su, Bilayer $t - J - J_\perp$ model and magnetically mediated pairing in the pressurized nickelate $\text{La}_3\text{Ni}_2\text{O}_7$, *Phys. Rev. Lett.* **132**, 036502 (2024).
- [46] Z. Luo, X. Hu, M. Wang, W. Wú, and D.-X. Yao, Bilayer two-orbital model of $\text{La}_3\text{Ni}_2\text{O}_7$ under pressure, *Phys. Rev. Lett.* **131**, 126001 (2023).
- [47] Y. Gu, C. Le, Z. Yang, X. Wu, and J. Hu, Effective model and pairing tendency in bilayer ni-based superconductor $\text{La}_3\text{Ni}_2\text{O}_7$, [arXiv:2306.07275](https://arxiv.org/abs/2306.07275).
- [48] H. Yang, H. Oh, and Y.-H. Zhang, Strong pairing from doping-induced feshbach resonance and second Fermi liquid through doping a bilayer spin-one Mott insulator: application to $\text{La}_3\text{Ni}_2\text{O}_7$, [arXiv:2309.15095](https://arxiv.org/abs/2309.15095).
- [49] H. Schlämer, U. Schollwöck, F. Grusdt, and A. Bohrdt, Superconductivity in the pressurized nickelate $\text{La}_3\text{Ni}_2\text{O}_7$ in the vicinity of a BEC-BCS crossover, [arXiv:2311.03349](https://arxiv.org/abs/2311.03349).
- [50] W. F. Brinkman and T. M. Rice, Single-particle excitations in magnetic insulators, *Phys. Rev. B* **2**, 1324 (1970).
- [51] S. A. Trugman, Interaction of holes in a Hubbard antiferromagnet and high-temperature superconductivity, *Phys. Rev. B* **37**, 1597 (1988).
- [52] P. Béran, D. Poilblanc, and R. B. Laughlin, Evidence for composite nature of quasiparticles in the 2D t-J model, *Nucl. Phys. B* **473**, 707 (1996).
- [53] R. B. Laughlin, Evidence for quasiparticle decay in photoemission from underdoped cuprates, *Phys. Rev. Lett.* **79**, 1726 (1997).
- [54] T. Senthil, S. Sachdev, and M. Vojta, Fractionalized Fermi liquids, *Phys. Rev. Lett.* **90**, 216403 (2003).
- [55] F. Grusdt, M. Kánász-Nagy, A. Bohrdt, C. S. Chiu, G. Ji, M. Greiner, D. Greif, and E. Demler, Parton theory of magnetic polarons: Mesonic resonances and signatures in dynamics, *Phys. Rev. X* **8**, 011046 (2018).
- [56] F. Grusdt, A. Bohrdt, and E. Demler, Microscopic spinon-chargon theory of magnetic polarons in the $t - J$ model, *Phys. Rev. B* **99**, 224422 (2019).
- [57] C. S. Chiu, G. Ji, A. Bohrdt, M. Xu, M. Knap, E. Demler, F. Grusdt, M. Greiner, and D. Greif, String patterns in the doped Hubbard model, *Science* **365**, 251 (2019).
- [58] S. R. White, Density matrix formulation for quantum renormalization groups, *Phys. Rev. Lett.* **69**, 2863 (1992).
- [59] U. Schollwöck, The density-matrix renormalization group in the age of matrix product states, *Ann. Phys. (NY)* **326**, 96 (2011).
- [60] H. Feshbach, Unified theory of nuclear reactions, *Ann. Phys. (NY)* **5**, 357 (1958).

- [61] H. Lange, L. Homeier, E. Demler, U. Schollwöck, F. Grusdt, and A. Bohrdt, Feshbach resonance in a strongly repulsive ladder of mixed dimensionality: A possible scenario for bilayer nickelate superconductors, *Phys. Rev. B* **109**, 045127 (2024).
- [62] See Supplemental Material at <http://link.aps.org/supplemental/10.1103/PhysRevB.110.L081113> for a discussion of the perturbative analysis for the low and high doping regimes, additional results on the bond-ordered density wave as well as information on the computation of the ARPES spectra.
- [63] C. Hubig, F. Lachenmaier, N.-O. Linden, T. Reinhard, L. Stenzel, A. Swoboda, and M. Grundner, The SYTEN toolkit, <https://syten.eu>.
- [64] C. Hubig, Symmetry-protected tensor networks, Ph.D. thesis, LMU München, 2017.
- [65] J. R. Schrieffer and P. A. Wolff, Relation between the anderson and kondo hamiltonians, *Phys. Rev.* **149**, 491 (1966).
- [66] S. Paeckel, T. Köhler, A. Swoboda, S. R. Manmana, U. Schollwöck, and C. Hubig, Time-evolution methods for matrix-product states, *Ann. Phys. (NY)* **411**, 167998 (2019).
- [67] T. Barthel, U. Schollwöck, and S. R. White, Spectral functions in one-dimensional quantum systems at finite temperature using the density matrix renormalization group, *Phys. Rev. B* **79**, 245101 (2009).
- [68] D. Chowdhury and S. Sachdev, The enigma of the pseudogap phase of the cuprate superconductors, in *Quantum Criticality in Condensed Matter* (World Scientific, Singapore, 2015), pp. 1–43.
- [69] L. Homeier, H. Lange, E. Demler, A. Bohrdt, and F. Grusdt, Feshbach hypothesis of high- T_c superconductivity in cuprates, [arXiv:2312.02982](https://arxiv.org/abs/2312.02982) [cond-mat.str-el].
- [70] J. N. Fuchs, A. Recati, and W. Zwerger, Exactly solvable model of the BCS-BEC crossover, *Phys. Rev. Lett.* **93**, 090408 (2004).
- [71] A. Recati, J. N. Fuchs, and W. Zwerger, Boson-fermion resonance model in one dimension, *Phys. Rev. A* **71**, 033630 (2005).
- [72] I. V. Tokatly, Dilute Fermi gas in quasi-one-dimensional traps: From weakly interacting fermions via hard core bosons to a weakly interacting bose gas, *Phys. Rev. Lett.* **93**, 090405 (2004).
- [73] R. Citro and E. Orignac, Atom-molecule coherence in a one-dimensional system, *Phys. Rev. Lett.* **95**, 130402 (2005).